

Laser-induced fluorescence detection of the elusive SiCF free radical

Cite as: J. Chem. Phys. **149**, 024301 (2018); <https://doi.org/10.1063/1.5040473>

Submitted: 17 May 2018 . Accepted: 19 June 2018 . Published Online: 09 July 2018

Gretchen Rothschof, Tony C. Smith , and Dennis J. Clouthier 



View Online



Export Citation



CrossMark

ARTICLES YOU MAY BE INTERESTED IN

Rovibrational analysis of c-SiC₂H₂: Further evidence for out-of-plane bending issues in correlated methods

The Journal of Chemical Physics **149**, 024303 (2018); <https://doi.org/10.1063/1.5043166>

Spectroscopy of gold atoms and gold oligomers in helium nanodroplets

The Journal of Chemical Physics **149**, 024305 (2018); <https://doi.org/10.1063/1.5026480>

Perspective: Basic understanding of condensed phases of matter via packing models

The Journal of Chemical Physics **149**, 020901 (2018); <https://doi.org/10.1063/1.5036657>





Lock-in Amplifiers



Zurich
Instruments

Watch the Video



Laser-induced fluorescence detection of the elusive SiCF free radical

Gretchen Rothschof,¹ Tony C. Smith,¹ and Dennis J. Clouthier^{2,a)}

¹*Ideal Vacuum Products, LLC, 5910 Midway Park Blvd. NE, Albuquerque, New Mexico 87109, USA*

²*Department of Chemistry, University of Kentucky, Lexington, Kentucky 40506-0055, USA*

(Received 17 May 2018; accepted 19 June 2018; published online 9 July 2018)

The SiCF free radical has been spectroscopically identified for the first time. The radical was produced in an electric discharge jet using $\text{CF}_3\text{Si}(\text{CH}_3)_3$ or CF_3SiH_3 vapor in high pressure argon as the precursor. The laser-induced fluorescence spectrum of the $\tilde{A}^2\Sigma^+ - \tilde{X}^2\Pi$ band system in the 610–550 nm region was recorded and the $^2\Pi_{3/2}$ spin component of the 0–0 band was studied at high resolution. Rotational analysis gave the B values for the combining states, and by fixing the CF bond lengths at *ab initio* values we obtained $r''(\text{Si}-\text{C}) = 1.692(1)\text{\AA}$ and $r'(\text{Si}-\text{C}) = 1.594(1)\text{\AA}$. The bond lengths correspond to a silicon-carbon double bond in the ground state and an unusual Si–C triple bond in the excited state. Single vibronic level emission spectra yielded the ground state bending and stretching energy levels. These were fitted to a Renner-Teller model that included spin-orbit and limited vibrational anharmonicity effects. Published by AIP Publishing. <https://doi.org/10.1063/1.5040473>

I. INTRODUCTION

In 2000, we identified the spectrum of the jet-cooled SiCH free radical for the first time.¹ This radical turned out to be quite interesting from several points of view. By detailed rotational analysis, we showed that SiCH has a silicon-carbon double bond in the ground state but this distance contracts by almost 0.1 Å on electronic excitation, forming a triple bond in the excited state. This odd occurrence is the result of promotion of a σ nonbonding electron from the ground state MO configuration $\dots\sigma_b^2\sigma_{nb}^2\pi^3$ to form an excited state $\dots\sigma_b^2\sigma_{nb}^1\pi^4$ configuration with 6 electrons in a $\sigma^2\pi^4$ triple bond. SiCH also has a $^2\Pi$ ground state which has significant spin-orbit, Renner-Teller, and Fermi resonance complications.²

Subsequently, we discovered the spectrum of GeCH which gave the first measure of the length of a germanium-carbon triple bond.³ The spin-orbit coupling constant in the Ge molecule is large (-388.3 cm^{-1}) and this leads to unusual complications in the Renner-Teller effect.⁴ The lower $\mu^2\Sigma_{1/2}$ component of the (0,1,0) level is very close to the upper $^2\Pi_{1/2}$ spin-orbit component of (0,0,0) and since they have the same value of $P = \Lambda + l$, they can interact, repelling each other through a process called Sears resonance. We were able to fit all of the observed ground state levels by expanding the Renner-Teller matrices to include such resonances.

In other work, we collaborated with Professor T. Steimle of Arizona State University to measure the dipole moments of SiCH and GeCH.^{5,6} Although SiCH is likely to be an important interstellar molecule, our measured ground state dipole moment of 0.066(2) D suggests that microwave and radioastronomy studies will be quite challenging. GeCH has measured dipole moments of $\mu(X^2\Pi) = 0.122(2)\text{ D}$ and

$\mu(\tilde{A}^2\Sigma^+) = 1.29(2)\text{ D}$ and the observed proton magnetic hyperfine splittings gave an upper state Fermi contact parameter of $b_F = 163(2)\text{ MHz}$.

In 2002, Evans and Clouthier used *ab initio* theory to predict the ground and excited state properties of the unknown silicon halomethylidyne (SiCX ; $X = \text{F, Cl, Br}$) free radicals.⁷ The ground state theoretical spin-orbit coupling constants, Renner parameters, and vibrational frequencies were used to generate energy level diagrams for the $\tilde{X}^2\Pi$ states as a guide to future experimental emission studies. In addition, the excited state excitation energies, molecular structures, and vibrational frequencies were used to simulate expected band contours for the 0–0 bands of the radicals under typical jet-cooled conditions. Subsequently, Smith, Evans, and Clouthier⁸ used these theoretical predictions to help find the spectrum of the SiCCl free radical and showed that the *ab initio* results agreed well with experiment.

Our theoretical predictions⁷ suggested that SiCF would be a good target for future studies, with a significant Renner-Teller effect in the ground state, a silicon-carbon triple bond in the excited state, no isotope complications, and resolvable rotational structure at high resolution. Over the intervening 15 years, we have made several attempts to record the spectrum of SiCF, but it has turned out to be much more elusive than expected. In the present work, we have finally succeeded in detecting SiCF through the $\tilde{A}^2\Sigma^+ - \tilde{X}^2\Pi$ LIF spectrum, have rotationally resolved the 0–0 band, have derived approximate ground and excited state molecular structures, and have obtained sufficiently resolved emission spectra to study the Renner-Teller effect in some detail.

II. EXPERIMENT

The SiCF reactive intermediate was generated by seeding the vapor of a suitable precursor into high pressure argon and subjecting pulses of this gas mixture to an electric discharge.

^{a)}Author to whom correspondence should be addressed: dclaser@uky.edu.

As described in detail elsewhere,^{9,10} a pulsed molecular beam valve (General Valve, series 9) injected the precursor mixture into a flow channel where an electric discharge between two stainless steel ring electrodes fragmented the precursor, producing the species of interest and a variety of other products. The reactive intermediates were rotationally and vibrationally cooled by free jet expansion into vacuum at the exit of the pulsed discharge apparatus. A 1.0 cm long reheat tube¹¹ added to the end of the discharge apparatus increased production of the SiCF radical and suppressed the background glow from excited argon atoms.

Moderate resolution (0.1 cm^{-1}) survey LIF spectra were recorded using a neodymium: yttrium aluminum garnet (Nd:YAG) pumped dye laser (Lumonics HD-500) excitation source. The fluorescence was collected by a lens, focused through appropriate longwave pass filters, onto the photocathode of a photomultiplier tube (RCA C31034A). The spectra were calibrated with optogalvanic lines from various argon- and neon-filled hollow cathode lamps to an estimated absolute accuracy of 0.1 cm^{-1} . The laser-induced fluorescence and calibration spectra were digitized and recorded simultaneously on a homebuilt computerized data acquisition system.

Higher resolution ($\sim 0.015\text{ cm}^{-1}$ FWHM) LIF spectra were obtained using a pulsed amplified ring dye laser (Coherent 699-21) as the excitation source using R590 dye. The linewidths in the LIF spectra were larger than that of the pulse amplified laser ($\sim 0.005\text{ cm}^{-1}$), primarily due to power broadening because of the necessity to use substantial laser intensity to obtain recordable LIF signals. Residual Doppler effects in the unskimmed beam also contributed to the linewidth. The amplifier was a Nd:YAG (532 nm) pumped 4-cell system of our own design which was operated with a mixture of R620 and R640 dyes. Absolute wavelength calibration of the CW ring laser, to an estimated accuracy of $\sim 0.001\text{ cm}^{-1}$, was performed by simultaneously recording the sub-Doppler absorption spectrum of a heated I_2 cell.¹² The IodineSpec5 program was used to calculate the hyperfine transition frequencies.¹³ Frequency calibration between the iodine lines was obtained by interpolation between transmission fringes through a pressure-stabilized confocal etalon (free spectral range FSR = 1.5 GHz) whose cavity length was actively locked to a frequency stabilized He—Ne laser.

For emission spectroscopy, previously measured LIF band maxima in the SiCF spectra were excited by the dye laser and the resulting fluorescence was imaged with $f/4$ optics onto the entrance slit of a 0.5 m scanning monochromator (Spex 500M). The pulsed fluorescence signals were detected with a gated CCD camera (Andor iStar 320T) and recorded digitally. The emission spectra were calibrated to an estimated accuracy of $\pm 1\text{ cm}^{-1}$ using emission lines from a neon lamp. A 1200 line/mm grating blazed at 750 nm was employed in this work, which gave a bandpass of 29.9 nm with 18 mm effective active area on the CCD. A spectral resolution of 0.2 nm was typical, depending on the signal intensity.

In order to untangle the weak SiCF LIF bands from the many impurity features, the emission setup was used in 2D-LIF mode, in which an emission spectrum was recorded for every

laser excitation wavenumber. A lower resolution 300 line/mm grating (blazed at 750 nm) was used with the gated CCD detector, the laser was incremented in steps of 0.2 cm^{-1} , and 200 shots were averaged for each laser step. The 120 nm detection region of the low resolution grating/CCD combination allowed us to record the major features of each emission spectrum without moving the grating. The LIF and emission wavenumbers were calibrated as before. Software was written to extract LIF spectra from user selected segments of the recorded emission spectra, effectively isolating the LIF bands of SiCF.

Trifluoromethyltrimethylsilane [$\text{CF}_3\text{Si}(\text{CH}_3)_3$, Aldrich, 95%], as received, was transferred to a Pyrex U-tube, degassed, pressured with 40–60 psi of argon, cooled to -15°C , and the gaseous mixture was used as a SiCF precursor. In addition, three other possible precursors were synthesized. Liquid (trifluoromethyl)trichlorosilane (CF_3SiCl_3) was obtained by the reaction of a $\text{CF}_3\text{Br} + \text{P}(\text{NEt}_2)_3$ complex with SiCl_4 in benzonitrile according to the method of Beckers *et al.*¹⁴ CF_3SiCl_3 was fluorinated by reaction with SbF_3 to produce gaseous (trifluoromethyl)trifluorosilane (CF_3SiF_3) or reduced with LiAlH_4 to yield gaseous trifluoromethylsilane (CF_3SiH_3).¹⁵ The purity of all three compounds was checked by gas phase infrared spectroscopy.^{14,15} These reactive compounds were stored at low temperatures in Pyrex U-tubes, pressurized with 40–60 psi of argon and delivered to the pulsed valve through stainless steel tubing.

III. RESULTS AND ANALYSIS

A. LIF spectra

Our previous theoretical study⁷ predicted the $^2\Pi_{3/2}$ spin component of the 0—0 band of SiCF to appear with an intense Q-branch at $\sim 17\,104\text{ cm}^{-1}$ [CCSD(T)/aug-cc-pVTZ] accompanied by a weaker transition from the upper spin-orbit component ($^2\Pi_{1/2}$) $80\text{--}93\text{ cm}^{-1}$ to lower energy. Under our typical experimental conditions, the LIF bands were predicted to be $15\text{--}20\text{ cm}^{-1}$ wide with possibly resolved rotational lines at either extreme. Armed with these expectations, we set out to search for the LIF spectrum using the commercially available $\text{CF}_3\text{Si}(\text{CH}_3)_3$ precursor. As shown in Fig. 1, this compound gives a very rich LIF spectrum in the target region, which our experience allowed us to readily identify as the spectra of HCF, SiH_2 , and SiCH_2 . However, among the weaker features, there were a few unidentified bands which matched our expectations for SiCF. Emission spectra (*vide infra*) of these bands were also promising, showing a pair of bands 665 and 770 cm^{-1} to the red of the excitation laser, giving a vibrational interval of 665 cm^{-1} and a splitting of 105 cm^{-1} , comparable to our *ab initio* predictions of $\nu_3'' = 685\text{--}639\text{ cm}^{-1}$ and spin-orbit coupling constant of $A = -80$ to -93 cm^{-1} . The pattern of bands suggested the 0—0 band should occur at lower energies, so we moved one dye to the red and recorded the spectrum shown in Fig. 2. The prominent LIF band at the center of the spectrum with Q-branch at $16\,571\text{ cm}^{-1}$ we assign as the $^2\Sigma^+ - ^2\Pi_{3/2}$ spin-orbit component of the 0—0 band of SiCF. Unfortunately, it is partially overlapped by known bands of the $\tilde{A}^1A_2 - \tilde{X}^1A_1$ system of SiCH_2 which we studied many years ago.¹⁶

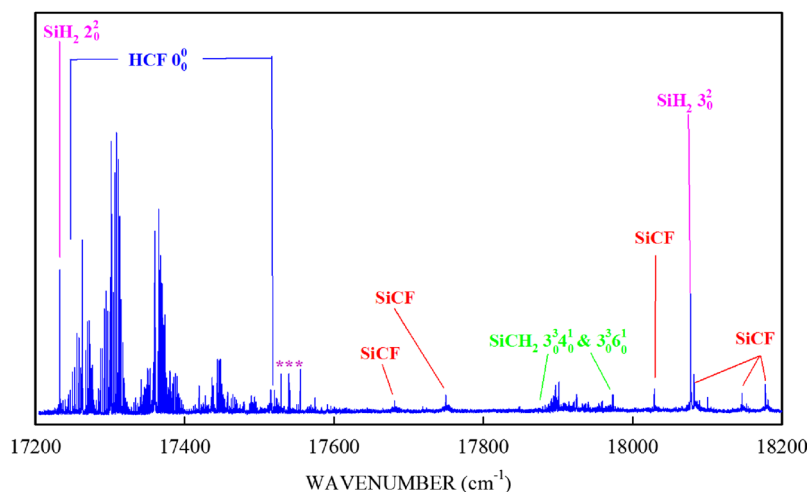


FIG. 1. A low resolution LIF spectrum of the products of an electrical discharge through $\text{CF}_3\text{Si}(\text{CH}_3)_3$ vapor diluted in argon. Most of the bands can be attributed to SiH_2 , HCF , and SiCH_2 but several weak bands with prominent Q-branches can be assigned as due to the SiCF free radical.

In an effort to clean up the spectrum, get rid of a lot of the extraneous impurity bands, and improve the LIF signal, we went to considerable trouble to synthesize alternate precursors which did not contain hydrogen. Of these, the most promising was CF_3SiF_3 which would seem ideally suited to produce SiCF . However, we could not find any experimental conditions which would give SiCF signals from this molecule, despite substantial effort. Mystified, we tried CF_3SiCl_3 , which we had in hand since it is the precursor to CF_3SiF_3 . The result was the same—no SiCF bands were observed. At this point, we theorized that the strong Si–F (135 kcal/mol), C–F (116 kcal/mol) and Si–Cl (90 kcal/mol) bonds¹⁷ in these molecules were hampering the discharge from producing SiCF . In CF_3SiCl_3 and CF_3SiF_3 with the plethora of electron withdrawing groups, the silicon-carbon bond is the weak link and they preferentially produce $\text{CF}_3 + \text{SiX}_3$ or perhaps $\text{CF}_2 + \text{SiX}_4$ as is observed thermally.¹⁸ In $\text{CF}_3\text{Si}(\text{CH}_3)_3$, the Si– CH_3 bonds are closer in energy to CF_3 –Si, so there is a small but finite chance of producing SiCF , as is observed experimentally. So we theorized that we needed a CF_3SiX_3

compound with readily eliminated X substituents. We settled on CF_3SiH_3 (Si–H bond strength ~ 75 kcal/mol) which was easily made by reducing CF_3SiCl_3 . The result, shown in Fig. 2, was positive— SiCF is made in a discharge through trifluoromethylsilane, the impurity spectra are different, but unfortunately the signals remained weak and rather unstable.

With two different precursors in hand, we continued experiments to prove that we had observed SiCF for the first time. Figure 3 shows the LIF spectrum of the 0–0 band in comparison to that calculated from our *ab initio* structures.⁷ It is clear that the observed band contour matches the prediction rather well, and the Q-branch is only $\sim 530\text{ cm}^{-1}$ lower in energy than our theoretical prediction, both factors providing good evidence that the spectra are due to SiCF .

Despite our substantial efforts at precursor development, the LIF spectra continued to be weak and overlapped by impurity bands. These difficulties were overcome using 2D-LIF spectroscopic techniques. Figure 4 shows an example of our success in extracting the positions of the 3_0^1 and 2_0^2 bands from

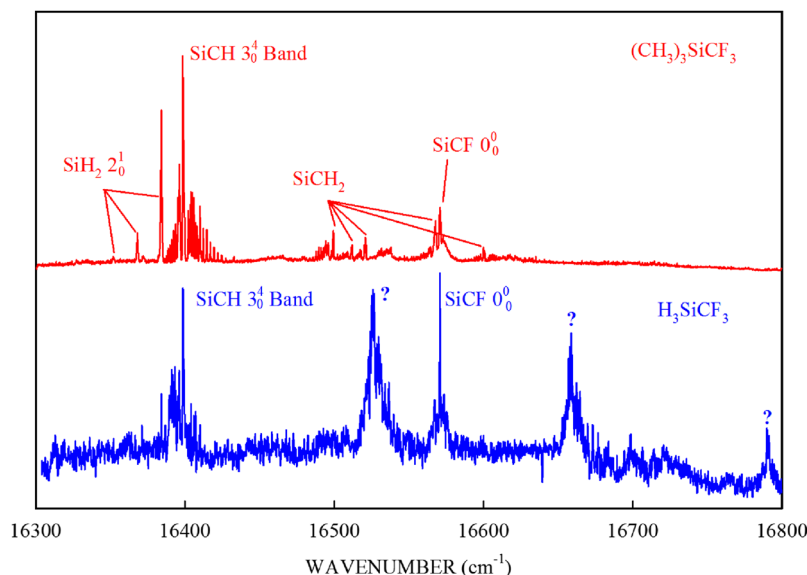


FIG. 2. Low resolution LIF spectra obtained with the $\text{CF}_3\text{Si}(\text{CH}_3)_3$ precursor (top) and the CF_3SiH_3 precursor (bottom). Bands marked ? are due to an unidentified impurity.

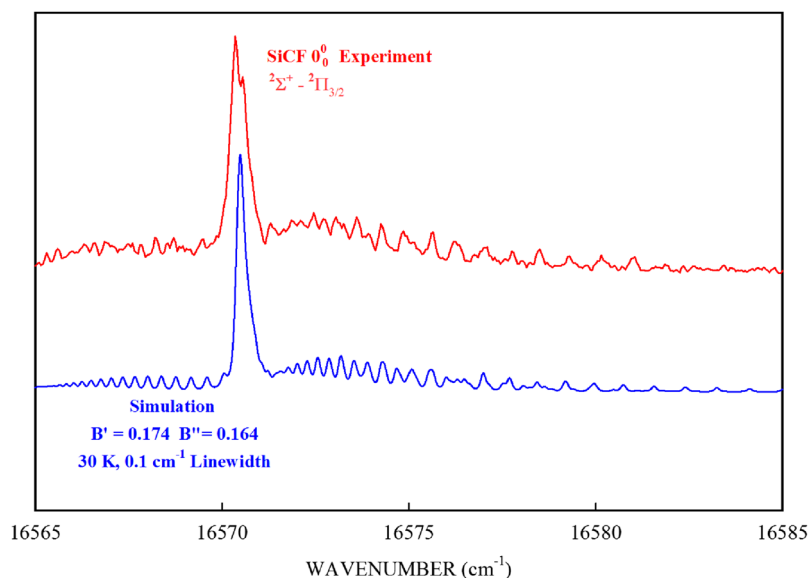


FIG. 3. A medium resolution scan of the 0–0 band of SiCF [top, $\text{CF}_3\text{Si}(\text{CH}_3)_3$ precursor] and our simulation of the band contour based on the *ab initio* geometries from Ref. 7.

the much stronger HCF features in this region (see Fig. 1). The bottom portion of Fig. 4 shows the 2D-LIF data as a color keyed plot with the excitation laser wavenumber (cm^{-1}) along the abscissa and the fluorescence displacement (laser wavenumber–emission wavenumber) along the ordinate. The fluorescence intensity is represented by color, with black being the most intense, fading through red, yellow, green, blue, and then white for the least intense, as shown by the color intensity scale along the right-hand side of the figure. The most intense black/bright red emission bands occur at 0 and 1410 cm^{-1} displacement and are readily assigned as HCF emission down to the 0_0 and 2_1 levels. In the present case, the much weaker SiCF emission spectra occur in regions between the HCF bands, predominantly from 490 to 700 cm^{-1} (2_2 band components at 492 and 644 cm^{-1} , *vide infra*) and 1700 to 2200 cm^{-1} (2_23_2 components). By setting these filter regions in software, the top SiCF LIF spectrum, substantially free of HCF features, was obtained and the bands were assigned based on their excited state intervals and emission spectra. Comparing Figs. 1 and 4, there is little evidence of these weak SiCF

bands in the total LIF spectrum but they are clearly apparent in the 2D scan. The 2D-LIF technique is a powerful tool which makes it possible to identify weak fluorescing species in regions where the spectrum is congested with overlapping band systems. Table I summarizes the Q-branch measurements and assignments for the observed SiCF LIF bands. The list is still somewhat limited due to the weakness of the spectra and persistent problems with overlapping impurity bands. We note that some bands in the table are formally forbidden, such as 2_0^1 . The occurrence of such vibronically induced bands following the selection rule $\Delta v_2 = \pm 1$ is not unexpected, as they are also prominent in the spectra of SiCH^1 and SiCCl^8 .

B. High resolution rotationally resolved spectra

Although our observed SiCF 0–0 LIF band is very weak, we fortunately were able to obtain a high resolution spectrum of the $2_2^1\Pi_{3/2}$ component. This involved concatenating a large number of individual 1 cm^{-1} ring laser scans, each individually

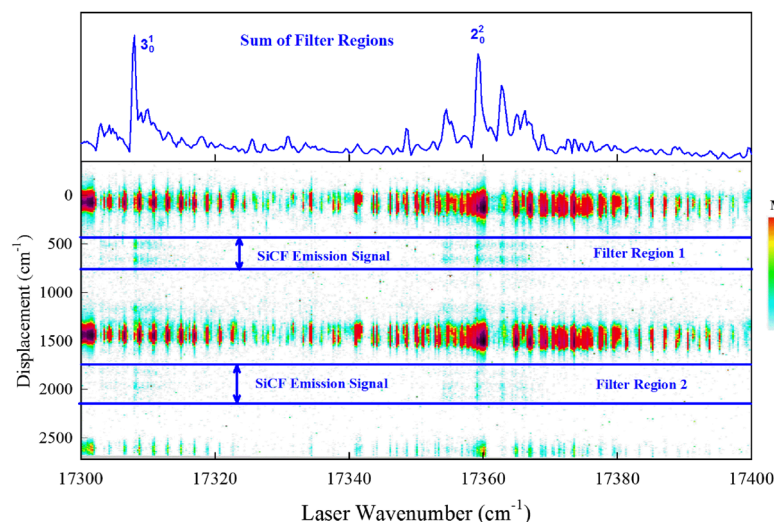


FIG. 4. A 2D-LIF spectrum of SiCF [$\text{CF}_3\text{Si}(\text{CH}_3)_3$ precursor] in the $17\,300$ – $17\,400\text{ cm}^{-1}$ region. The excitation wavenumber of the laser is given along the abscissa and the emission spectrum at each laser position is given along the ordinate. The emission spectra are plotted as displacement from the laser position, which gives a direct measure of the ground state energy of each transition, and the intensities are color coded (see the legend on the RHS). By setting two filter regions and combining their intensities in software, the 2D-LIF spectrum of SiCF (top trace) was obtained, almost completely eliminating the impurity emission from HCF (see Fig. 1).

TABLE I. Assignments and Q-branch maxima of the observed bands (all values in cm^{-1}) in the LIF spectrum of SiCF.

Assign.	$^2\Pi_{3/2}$	$^2\Pi_{1/2}$	Comment
0_0^0	16571.0	16465.8	$\Delta_{\text{so}} = -105.2$
2_0^1	16958.9	16853.7	$\Delta_{\text{so}} = -105.2$ $\nu'_2 = 387.9$
3_0^1	17308.1	...	$\nu'_3 = 737.1$
2_0^2	17359.2	...	$2_0^1 + 400.3$
$2_0^1 3_0^1$	17680.9	...	$2_0^1 + 722.0$
2_0^3	17749.7	...	$2_0^2 + 390.5$
3_0^2	18029.2	...	$3_0^1 + 721.1$
$2_0^2 3_0^1$	18082.3	...	$2_0^2 + 723.1$
2_0^4	18146.5	...	$2_0^3 + 396.8$
1_0^1	18177.9	...	$\nu'_1 = 1606.9$

calibrated, to obtain the spectrum shown in Fig. 5. Although the central Q branch features are not well-resolved, the branches on either side show clearly delineated rotational lines. Figure 6 shows a small portion of the high resolution spectrum in the region near the onset of the R_{21} branch. The J -dependent upper state spin-rotation splittings evident as the difference of the $Q_{21}(J'')$ and $R_{11}(J'')$ lines are also illustrated.

We have fitted the rotational structure of our spectrum using the very convenient graphical PGopher program.^{19,20} Since only one spin component was observed, we fixed the lower state spin-orbit coupling constant A at the value of -105.2 cm^{-1} obtained from the low resolution data (Table I). Our starting point was to use the predicted rotational constants obtained in our previous *ab initio* work⁷ to simulate the spectrum (see Fig. 3) which allowed us to assign lines in the resolved branches with relative ease. Initially, we only fitted the two B values and the band origin, adding the excited state spin-rotation constant γ as needed to fit the higher J' Q_{21} and R_{11} lines. It was soon evident that the

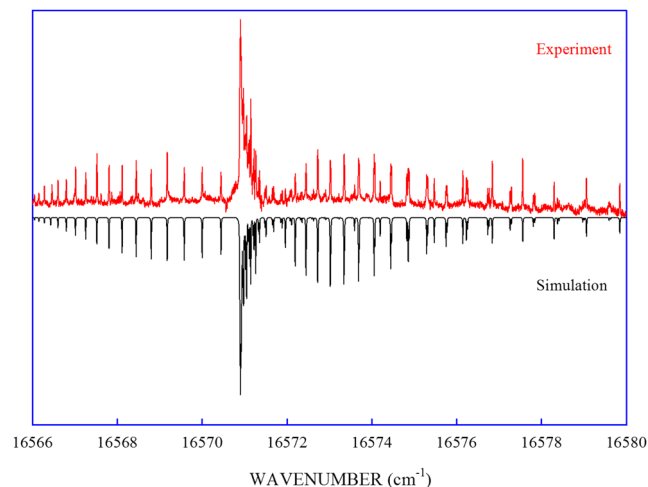


FIG. 5. The high resolution spectrum of the $^2\Pi_{3/2}$ component of the 0—0 band of SiCF [top, $\text{CF}_3\text{Si}(\text{CH}_3)_3$ precursor] and the simulation of the spectrum at a rotational temperature of 20 K (bottom). The experimental spectrum was obtained by concatenating 15 individual 1 cm^{-1} scans with varying laser power and experimental conditions, accounting for the irregularity in the baseline. Some weaker features in the spectra not reproduced in the simulation are due to impurity fluorescence.

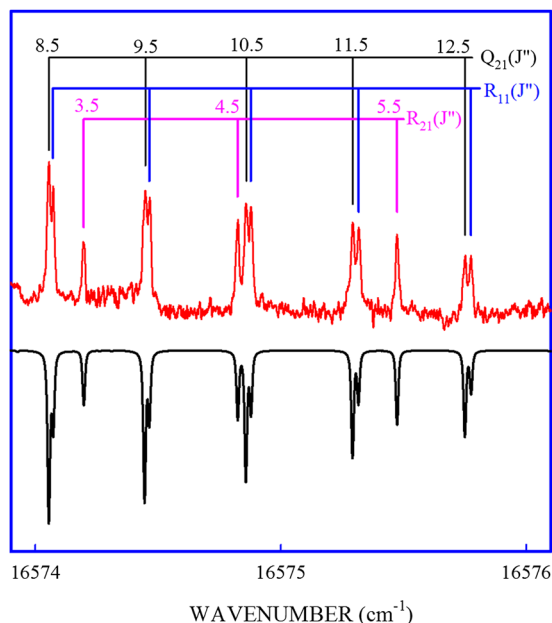


FIG. 6. A small portion of the high resolution spectrum of the $^2\Pi_{3/2}$ component of the 0—0 band of SiCF [top, $\text{CF}_3\text{Si}(\text{CH}_3)_3$ precursor] showing the onset of resolved spin-rotation splittings [$R_{11}(J'')$ – $Q_{21}(J'')$] and the R_{21} branch lines. The simulation (bottom) was obtained using the constants in Table III and a rotational temperature of 20 K.

ground state Λ doubling was negligible at our resolution and that the centrifugal distortion constants (D) were not determinable in either state. In the final analysis, we used 5 constants to fit 68 transitions to an overall standard deviation of 0.0015 cm^{-1} , with the results summarized in Tables II and III. The $P_{11}(15.5)$ line was left out of the analysis and it is not listed in Table II, as it was found that the scan segment had a mode hop which invalidated the line frequency determination. Simulations of the spectra using the fitted constants and an estimated rotational temperature of 20 K are shown in Figs. 5 and 6, illustrating good agreement with the line positions and reasonable reproduction of the relative intensities. No perturbations were detected in any of the branches of the spectrum.

C. Emission spectra

By extensive signal averaging (20 000 laser shots), we were able to obtain good emission spectra from laser excitation of the $^2\Pi_{3/2}$ spin-orbit components of the 0_0^0 and 2_0^1 bands, as illustrated in Fig. 7. The figure also shows the calculated energy level pattern for the ground state, derived from our previous *ab initio* study.⁷ The 0—0 band emission spectrum is quite simple, consists of transitions down to the two spin-orbit components of the zero-point level (the gated CCD allows us to gate out all of the scattered laser light), a second doublet at $666/770 \text{ cm}^{-1}$ assigned as 3_1^0 , and a similar 3_2^0 band at $1334/1431 \text{ cm}^{-1}$. The spin-orbit intervals are $105 \text{ cm}^{-1}(000)$, $104 \text{ cm}^{-1}(001)$, and $97 \text{ cm}^{-1}(002)$. As is evident from the figure, the smaller spin-orbit splitting in (002) is readily explained by a Fermi resonance interaction with the nearby (021) level, accounting for the intensity of the transition to the latter in the emission spectrum. We were also able to assign transitions to

TABLE II. Rotational line frequencies (cm^{-1}) and assignments for the $2\Sigma^+ - 2\Pi_{3/2}$ component of the 0–0 band of SiCF.

J''	R_{21}	R_{11}	Q_{21}	Q_{11}	P_{21}	P_{11}
1.5		*16571.9629(−30) ^a	*16571.9629(18)			
2.5	16573.5943(17)	*16572.1938(−52)	*16572.1938(16)			16570.4431(−14)
3.5	16574.1967(−1)	*16572.4486(−60)	*16572.4486(26)			16569.9992(−2)
4.5	16574.8237(−1)	*16572.7257(−73)	*16572.7257(32)			16569.5757(−11)
5.5	16575.4738(6)	*16573.0250(−90)	*16573.0250(34)			16569.1749(−21)
6.5	16576.1467(−12)	*16573.3481(−97)	*16573.3481(47)			16568.7992(−7)
7.5	16576.8406(2)	*16573.6938(−104)	*16573.6938(59)			16568.4443(−12)
8.5	16577.5579(−2)	16574.0710(−18)	16574.0549(1)			16568.1140(2)
9.5	16578.2991(6)	16574.4636(−11)	16574.4483(35)			16567.8040(−7)
10.5	16579.0606(−9)	16574.8778(−15)	16574.8601(27)	*16571.0245(10)	16571.0021(−15)	16567.5192(8)
11.5	16579.8471(−3)	16575.3172(7)	16575.2937(10)	*16571.1112(9)	*16571.0901(16)	16567.2548(−1)
12.5	16580.6555(−3)	16575.7739(−26)	16575.7501(−7)	*16571.2225(27)	*16571.2023(62)	16567.0147(8)
13.5	16581.4880(10)	16576.2599(8)	16576.2315(−1)	16571.3546(24)	16571.3288(22)	16566.7952(−5)
14.5	16582.3389(−20)	16576.7659(14)	16576.7347(−10)	16571.5053(−18)	16571.4802(6)	16566.5997(−5)
15.5		16577.2928(3)	16577.2602(−9)	16571.6831(−17)	16571.6554(1)	...
16.5		16577.8448(16)	16577.8108(8)	16571.8855(4)	16571.8550(12)	16566.2785(12)
17.5		16578.4190(23)	16578.3803(−13)	16572.1050(−31)	16572.0754(−5)	16566.1496(−4)
18.5		16579.0144(15)	16578.9731(−27)	16572.3539(−2)	16572.3209(22)	16566.0476(24)
19.5				16572.6253(30)	16572.5857(4)	16565.9627(−6)
20.5				16572.9106(−28)	16572.8717(−28)	

^aThe numbers in parentheses are observed minus calculated values in units of 10^{-4} cm^{-1} . An asterisk denotes a blended or otherwise poor line not used in the least squares fitting.

both spin-orbit components of the 1_1^0 band at the very end of the spectrum.

The 2_1^0 band emission spectrum is almost completely different, which is expected from the selection rules and fortunate as the observed transitions basically define the Renner-Teller problem. There is weak resonance fluorescence down to the $(000) 2\Pi_{3/2}$ level, coincident with the laser wavelength, and then a strong group of four lines down to (010) which satisfy the $\Delta v_2 = 0$ selection rule. This pattern is repeated for transitions down to (011) .

We have fitted our data to a Renner-Teller model including spin-orbit and Fermi resonance complications using a computer program²¹ written especially for this purpose and employed previously to analyze similar emission data for SiCH,² GeCH,⁴ and SiCCl.⁸ We were able to fit the 18 observed ground state energy levels with a minimal set of constants including $\omega_1, \omega_2, \omega_3, \varepsilon\omega_2, g_k, A$ and the x_{23} anharmonicity constant, to an overall standard deviation of 2.24 cm^{-1} , which is very satisfactory for a Renner-Teller analysis. Although there is evidence of Fermi resonance in the spectrum, neither of the Fermi resonance parameters W_1 or W_2 were determinable by least squares due to an insufficiency

of data on the higher energy levels. The fitted levels and their least squares residuals are given in Table IV and the resulting constants are summarized in Table V.

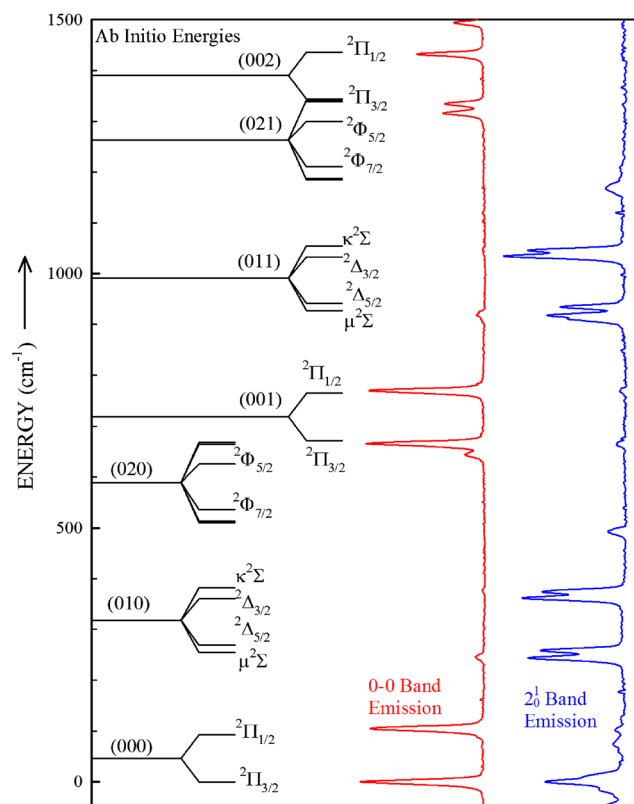


FIG. 7. The emission spectra observed from laser excitation of the $2\Pi_{3/2}$ spin-orbit components of the 0_0^0 and 2_1^0 bands of SiCF [$\text{CF}_3\text{Si}(\text{CH}_3)_3$ precursor]. The vertical scale is displacement from the excitation laser wavenumber, giving a direct measure of the relative ground state energy of each transition. The corresponding energy levels obtained from our *ab initio* study (Ref. 7) are given on the left-hand side.

TABLE III. The molecular constants (in cm^{-1}) of SiCF.

Parameter	2Π	$2\Sigma^+$
T_0	...	16 518.804 ₁ (1)
B	0.164116 ₂ (25) ^a	0.175212 ₇ (26)
A	−105.2 ^b	...
γ	...	0.00190(9)

^aThe numbers in parentheses are 3 σ error limits and are right-justified to the last digit on the line; sufficient additional digits are quoted to reproduce the original data to full accuracy. 68 transitions were fitted with an overall standard deviation of 0.0015 cm^{-1} .

^bValue taken from Table I and fixed in the least squares fitting.

TABLE IV. Vibrational levels of the $\tilde{X}^2\Pi_i$ state of SiCF [in cm^{-1} relative to the lowest (000) $^2\Pi_{3/2}$ level].

State ($v_1v_2v_3$)	Energy	Obs. – Calc. ^a
(000) $^2\Pi_{1/2}$	105	1.94
(010) $\mu^2\Sigma$	244	–0.08
(010) $^2\Delta_{5/2}$	259	–1.33
(010) $^2\Delta_{3/2}$	361	–1.13
(010) $\kappa^2\Sigma$	374	1.22
(020) $\mu^2\Pi_{3/2}$	492	–1.43
(020) $\kappa^2\Pi_{3/2}$	644	2.10
(001) $\mu^2\Pi_{3/2}$	666	–0.19
(001) $\kappa^2\Pi_{1/2}$	770	0.72
(011) $\mu^2\Sigma$	918	2.16
(011) $^2\Delta_{5/2}$	935	2.87
(011) $^2\Delta_{3/2}$	1035	0.98
(011) $\kappa^2\Sigma$	1045	0.44
(021) $\kappa^2\Pi_{3/2}$	1316	–3.23
(002) $^2\Pi_{3/2}$	1334	1.62
(002) $^2\Pi_{1/2}$	1432	–3.50
(100) $^2\Pi_{3/2}$	1494	–0.47
(100) $^2\Pi_{1/2}$	1598	0.47

^aFrom our Renner-Teller analysis of the emission spectra.

IV. DISCUSSION

A. The molecular structure of SiCF

With only a single B value for each state, it is not possible to completely determine the molecular structure of the SiCF radical. However, if we constrain the CF bond lengths to our *ab initio* values,⁷ we can get approximate SiC bond lengths of $r'' = 1.692(1)$ and $r'1.594(1)$ Å, as summarized in Table V. Theory predicts a 0.1 Å decrease in the SiC bond length on electronic excitation, mirrored almost exactly by the 0.098 Å value obtained from the rotational constants. Since the change in the CF bond length is predicted to be miniscule (+0.008 Å) on electronic excitation, it is unlikely that any over- or underestimation of the carbon-halogen bond length can substantially affect the experimentally derived decrease in the Si–C bond length. It is evident that the SiCF bond order

increases substantially on electronic excitation, precisely as found from purely experimental structures derived previously for SiCH¹ and GeCH.³

These results can be readily understood from the molecular orbitals (MOs) involved. In the ground state of SiCF, the electron configuration is $\dots(\sigma_b)^2(\sigma_{nb})^2(\pi)^3(^2\Pi)$, where σ_b is an Si–C bonding orbital, σ_{nb} is a nonbonding lone pair on the silicon atom, and the π orbitals are Si–C bonding. In both SiCH¹ and SiCF, the resulting SiC bond length is 1.693 ± 0.001 Å, which can be interpreted as a carbon-silicon double bond. Clearly, halogen substitution onto SiCH has little effect on this bond. The first electronic excited state is formed by promotion of an electron from the nonbonding orbital to the π bonding orbitals, yielding the configuration $\dots(\sigma_b)^2(\sigma_{nb})^1(\pi)^4(^2\Sigma^+)$ which now has a total of six electrons in bonding orbitals, forming a carbon-silicon triple bond. In SiCF, the bond length is $1.594(1)$ Å, analogous to the $1.6118(1)$ Å bond length in excited SiCH,¹ precisely as predicted by *ab initio* theory.⁷

We can also compare the Si–C bond lengths of SiCF to those reported in the literature for other compounds. Silicon-carbon single bonds are much longer, of the order of 1.87–1.91 Å.²² We determined the length of the silicon-carbon double bond in transient silylidene ($\text{H}_2\text{C}=\text{Si}$)²³ to be 1.706 Å, very similar to the 1.7039 Å value in highly reactive gas phase $\text{H}_2\text{Si}=\text{CH}_2$,^{24,25} and both only 0.014–0.012 Å longer than that of the SiCF. Several stable silicon–carbon doubly bonded molecules have also been reported.²² These invariably have large bulky substituents to tame their inherent reactivity, with typical bond lengths ranging from 1.702–1.764 Å. To our knowledge, there are no known stable molecules with carbon-silicon triple bonds, but theory predicts a value of 1.604 Å for linear $\text{HC}\equiv\text{SiH}$,²⁶ very close to the excited state value obtained for SiCF.

B. Rotational and vibrational analysis

The observed $^2\Pi$ state spin-orbit coupling splitting in SiCF (-105.2 cm^{-1}) is somewhat larger than the -80 to -93 cm^{-1} values predicted in our *ab initio* study, similar to the

TABLE V. Experimental and *ab initio* spectroscopic parameters of SiCF.

Parameter	$\tilde{X}^2\Pi$		$\tilde{A}^2\Sigma^+$	
	Experiment	<i>Ab Initio</i>	Experiment	<i>Ab Initio</i>
T_0 cm^{-1}	0	0	16 518.804(1)	17 104 ^a
ω_1 (C–F stretch) cm^{-1}	1494.5(17) ^b	1454 ^c	1606.9 ^d	1595 ^c
ω_2 (bend) cm^{-1}	259.83(82) ^b	250	387.9	408
ω_3 (Si–C stretch) cm^{-1}	666.17(78) ^b	640	737.1	749
x_{23}	5.57(121) ^b
ϵ	–0.148(5) ^b	–0.199
Spin-orbit coupling constant, A , cm^{-1}	–103.68(112) ^b	–93
C–F bond length (Å)	...	1.288 ^e	...	1.296 ^e
SiC bond length (Å)	1.692(1)	1.703 ^e	1.594(1)	1.602 ^e

^a T_0 calculated from CCSD(T)/aug-cc-pVTZ T_e and G96LYP/aug-cc-pVTZ frequencies, Ref. 7.^bFrom our Renner-Teller analysis of the emission spectra. The numbers in parenthesis are 1 σ standard errors.^cG96LYP/aug-cc-pVTZ values, Ref. 7.^dVibrational fundamental by subtracting Q-branch maxima from Table I.^eCCSD(T)/aug-cc-pVTZ values, Ref. 7.

underestimation in SiCCl (-115 cm^{-1} theory vs -159.4 cm^{-1} experiment). In the pure precession approximation, the predominant contribution to the excited state spin-rotation parameter γ would come from the interaction with the $^2\Pi_i$ ground state, given by the relation

$$\gamma = 2ABl(l+1)/(E_{\Pi} - E_{\Sigma}), \quad (1)$$

where A is the spin-orbit coupling constant, l is the angular momentum quantum number of the electron that gives rise to the Σ and Π states, and B is the rotational constant of the Σ state. The calculated value is $4.46 \times 10^{-3}\text{ cm}^{-1}$ compared to $\gamma = 1.9 \times 10^{-3}\text{ cm}^{-1}$ determined experimentally, agreeing in sign but differing substantially in magnitude, as was found previously for SiCH.¹

As summarized in Table V and Fig. 7, the *ab initio* predictions of the ground state vibrational and Renner-Teller parameters are in gratifyingly good agreement with experiment. As discussed previously,⁷ the stretching frequencies are anomalous, with ω_3 (nominal SiC stretch) = 666 cm^{-1} much lower than the 1175 cm^{-1} and 1275 cm^{-1} values for SiCH and SiCCl, respectively. This is because, in SiCF, the two stretching modes are not distinct, but are rather admixtures of the stretching internal coordinates and behave as the symmetric and antisymmetric stretching motions of a symmetric triatomic molecule. The bending frequency and Renner-Teller parameter are as expected from theory, and the predicted ground state energy level pattern including the Renner-Teller and spin-orbit effects (see Fig. 6) was very useful in understanding the emission spectra.

As reproduced by our *ab initio* calculations, substitution of more electronegative halogen substituents onto SiCH shifts the band origin of the $^2\Sigma^+ - ^2\Pi$ electronic transition substantially to the blue (SiCH = 11766.7 cm^{-1} , SiCCl = 15164 cm^{-1} , SiCF = 16518.8 cm^{-1}). Our CCSD(T)/aug-cc-pVTZ results⁷ overestimate the T_0 values by $300\text{--}800\text{ cm}^{-1}$, while the ground state spin-orbit constants are underestimated by 5% (SiCH) to 28% (SiCCl). As shown in Fig. 3, the *ab initio* rotational constants are gratifyingly good at reproducing the low resolution contour of the SiCF 0–0 band.

The derived excited state vibrational frequencies of SiCF are compared to our previous *ab initio* values⁷ in Table V. The agreement is excellent and lends confidence to the assignments of the weak LIF bands. We note that the emission spectra of the 3_0^1 and 2_0^2 bands (Fig. 4) are very similar and involve primarily activity in $2\nu_2''$, whereas we expected 3_0^1 would emit more strongly down to ν_3'' . This initially cast some doubt on which LIF band was which, but the current assignments are the most consistent with the *ab initio* frequencies. Since 3^1 and 2^2 are only 50 cm^{-1} apart, it is likely that the levels are in Fermi resonance, accounting for the similarity in their emission spectra.

V. CONCLUSIONS

After considerable effort, the SiCF free radical has been detected in the gas phase. Although CF_3SiF_3 did not produce SiCF in our electric discharge jet, $\text{CF}_3\text{Si}(\text{CH}_3)_3$ and CF_3SiH_3 were found to be viable precursors that gave weak spectra

that were positively attributable to the previously unknown SiCF species. High resolution rotationally resolved spectra of the 0–0 band allowed a determination of the linear molecule silicon-carbon bond lengths as $r''(\text{Si}-\text{C}) = 1.692(1)\text{ \AA}$ and $r'(\text{Si}-\text{C}) = 1.594(1)\text{ \AA}$ with $r(\text{C}-\text{F})$ fixed at *ab initio* values. Using 2D-LIF and single vibronic level emission techniques, several LIF bands of SiCF were identified amidst a host of stronger signals from impurities produced in the discharge. In addition, the resolved emission spectra from the 0^0 and 2^1 levels were fitted to a Renner-Teller model, allowing the elucidation of the vibrational angular momentum coupling and spin-orbit effects in the ground state.

ACKNOWLEDGMENTS

T.C.S. thanks Professor T. Steimle for valuable advice and support in the implementation of the 2D-LIF and high resolution laser techniques. D.J.C. is very grateful to the staff of Ideal Vacuum Products LLC for making his sabbatical leave in Albuquerque in the spring of 2017 such an enjoyable and productive time. D.J.C. also thanks the students, faculty, and staff at the University of Kentucky for 34 years of stimulating opportunities in teaching and research. The authors thank Dr. Mohammed Gharaibeh of the Department of Chemistry, University of Jordan for efforts at the University of Kentucky to identify the weak SiCF LIF bands. This research was funded by Ideal Vacuum Products.

¹T. C. Smith, H. Li, D. J. Clouthier, C. T. Kingston, and A. J. Merer, *J. Chem. Phys.* **112**, 3662 (2000).

²T. C. Smith, H. Li, D. A. Hostutler, D. J. Clouthier, and A. J. Merer, *J. Chem. Phys.* **114**, 725 (2001).

³T. C. Smith, H. Li, D. J. Clouthier, C. T. Kingston, and A. J. Merer, *J. Chem. Phys.* **112**, 8417 (2000).

⁴S. He, H. Li, T. C. Smith, D. J. Clouthier, and A. J. Merer, *J. Chem. Phys.* **119**, 10115 (2003).

⁵T. C. Smith, D. J. Clouthier, and T. C. Steimle, *J. Chem. Phys.* **115**, 817 (2001).

⁶T. C. Smith, D. J. Clouthier, and T. C. Steimle, *J. Chem. Phys.* **115**, 5047 (2001).

⁷C. J. Evans and D. J. Clouthier, *J. Chem. Phys.* **117**, 6439 (2002).

⁸T. C. Smith, C. J. Evans, and D. J. Clouthier, *J. Chem. Phys.* **117**, 6446 (2002).

⁹H. Harjanto, W. W. Harper, and D. J. Clouthier, *J. Chem. Phys.* **105**, 10189 (1996).

¹⁰W. W. Harper and D. J. Clouthier, *J. Chem. Phys.* **106**, 9461 (1997).

¹¹D. L. Michalopoulos, M. E. Geusic, P. R. R. Langridge-Smith, and R. E. Smalley, *J. Chem. Phys.* **80**, 3556 (1984).

¹²S. Gerstenkorn and P. Luc, *Atlas du Spectre D'Absorption de la Molecule d'Iode* (Editions du CNRS, Paris, 1978); *Rev. Phys. Appl.* **14**, 791 (1979).

¹³H. Knoeckel and E. Tiemann, Program IodineSpec5, <http://www.iqo.uni-hannover.de>.

¹⁴H. Beckers, H. Burger, P. Bursch, and I. Ruppert, *J. Organomet. Chem.* **316**, 41 (1986).

¹⁵H. Beckers, H. Burger, and R. Eujen, *J. Fluorine Chem.* **27**, 461 (1985).

¹⁶T. C. Smith, C. J. Evans, and D. J. Clouthier, *J. Chem. Phys.* **118**, 1642 (2003).

¹⁷See http://www.wiredchemist.com/chemistry/data/bond_energies_lengths.html for a table of typical bond lengths.

¹⁸H. Burger, R. Eujen, and P. Moritz, *J. Organomet. Chem.* **401**, 249 (1991).

¹⁹See <http://pgopher.chm.bris.ac.uk> for PGOPHER, a Program for Simulating Rotational Structure, C. M. Western, University of Bristol.

²⁰C. M. Western, "PGOPHER: A program for simulating rotational, vibrational and electronic spectra," *J. Quant. Spectrosc. Radiat. Transfer* **186**, 221–242 (2016).

- ²¹S. G. He and D. J. Clouthier, [Comput. Phys. Commun.](#) **178**, 676 (2008).
- ²²P. P. Power, [Chem. Rev.](#) **99**, 3463 (1999).
- ²³W. W. Harper, K. W. Waddell, and D. J. Clouthier, [J. Chem. Phys.](#) **107**, 8829 (1997).
- ²⁴S. Bailleux, M. Bogey, J. Breidung, H. Burger, R. Fajgar, Y. Liu, J. Pola, M. Senzlober, and W. Thiel, [Angew. Chem., Int. Ed. Engl.](#) **35**, 2513 (1996).
- ²⁵S. Bailleux, M. Bogey, J. Demaison, H. Burger, M. Senzlober, J. Breidung, W. Thiel, R. Fajgar, and J. Pola, [J. Chem. Phys.](#) **106**, 10016 (1997).
- ²⁶R. Stegmann and G. Frenking, [J. Comput. Chem.](#) **17**, 781 (1996).